ASYMPTOTIC AND NUMERICAL METHODS FOR SOLVING BURGER'S EQUATION

F. H. Fenlon

ABSTRACT

First, a review of the approximations involved in deriving Burger's equation from the conservation equations is given. This discussion is then followed by an assessment of the asymptotic methods which have been used to obtain exact solutions for particular source waveforms. Finally, numerical and approximate methods for solving Burger's equation are compared. In particular, a technique developed by the author for replacing Burger's equation by a coupled set of ordinary nonlinear differential equations, which provides a complete description of nonlinear mode conversion for arbitrary source waveforms, is discussed in some detail.

INTRODUCTION

As discussed by Beyer,[1] Burger's equation, which is well known in aerodynamics, was first introduced into acoustics by Mendousse[2] in 1953 for studying the propagation of finite-amplitude waves. Since then it has been extensively analyzed by Naugolnykh, Soluyan and Khokhlov[3-6] in the Soviet Union, and by Blackstock[7-11] in the United States. Thus, in order to put the work carried out during the past eighteen years in perspective, the major contributions, both analytical and numerical, which have been made to date will be briefly reviewed, following which a technique developed by the author for solving Burger's equation with arbitrary source waveforms will be considered.

In order to introduce Burger's equation and the assumptions on which it is based we will consider a simplified derivation of this equation from the conservation equations of mass and momentum together with the equation of state. These equations are shown in Fig. 1, where ρ is the instantaneous density in the

Conservation of Mass: -

$$\frac{\partial \rho}{\partial t} + \frac{\partial (\rho v_i)}{\partial x_i} = 0$$

Conservation of Momentum: -

$$\frac{\partial (\rho v_i)}{\partial t} + \frac{\partial \pi_{ij}}{\partial x_j} = 0$$

Equation of State: -

$$p = p_0 + A\left[\rho'/\rho_0\right] + \frac{B}{2}\left[\rho'/\rho_0{}^2\right]$$

$$\pi_{ij} = \rho v_i v_j + p\,\delta_{ij} - (\eta + \eta')\frac{\partial v_j}{\partial x_i} - \eta\frac{\partial v_i}{\partial x_j}$$

$$\rho' = \rho - \rho_0$$

$$A = \rho_0\left(\frac{\partial p}{\partial \rho}\right)_{s,\ \rho = \rho_0} = \rho_0 c_0{}^2$$

$$B = \rho_0{}^2\left(\frac{\partial^2 p}{\partial \rho^2}\right)_{s,\ \rho = \rho_0}$$

Fig. 1

medium p is the instantaneous pressure, v is the particle velocity, and the subscripts i and j are used to identify the spatial variables in the standard notation adopted by Landau and Lifshitz[12]. The term π_{ij} represents the momentum-flux-density tensor, which in this instance is quite general and includes both inertial and viscous terms. The parameters B and A which appear in the equation-of-state are well known in finite-amplitude acoustics and are defined below. Now since we are only going to include second order terms in the equation-of-state, we are therefore restricted to Mach numbers less than 0.1 (which corresponds to a sound-pressure level of 187 dB re 1 μ bar in water). Consequently, following Lighthill[13], we can assert that even if weak shocks are formed in the medium, the change in entropy across the shock front is of the third order in the Mach number, and can therefore be neglected. Thus we are considering an essentially isentropic process, which justifies our exclusion of the energy-balance equation. Differentiating the equation of Mass-conservation therefore, with respect to time, and the conservation of momentum equation with respect to x_i, and making use of the equation of state to eliminate the pressure term, we can deduce the general form of the second order nonlinear wave equation in a matter of a few lines. This equation is shown in the upper portion of Fig. 2 and below it is its one dimensional counterpart. In order to reduce this equation we make use of a transformation introduced by Khokhlov[14] in the analysis of electric signals on nonlinear transmission lines where the rate of nonlinear generation and dissipation per wavelength of propagation path are assumed to be small. The essence of this transformation is represented schematically in Fig. 3, where it is to be understood that the rate-of-change of the waveform with respect to the spatial variable is considerably less

Dwg. 2942A85

$$\frac{\partial^2 \rho}{\partial t^2} - c_o^2 \nabla^2 \rho - \left[(2\eta + \eta')/\rho_o\right] \nabla^2 \left(\frac{\partial \rho}{\partial t}\right) = \frac{\partial^2}{\partial x_i \partial x_j} \left[\rho v_i v_j + \frac{B}{2} (p'/\rho_o)^2\right]$$

In One Dimension: –

$$\frac{\partial^2 \rho}{\partial t^2} - c_o^2 \frac{\partial^2 \rho}{\partial x^2} - \left[(2\eta + \eta')/\rho_o\right] \frac{\partial^3 \rho}{\partial x^2 \partial t} = \frac{\partial^2}{\partial x^2} \left[\rho v^2 + \frac{B}{2} (p'/\rho_o)^2\right]$$

Fig. 2

Dwg. 2942A95

Khokhlov Transformation:

$$x \to \zeta = x \quad ; \quad \frac{\partial}{\partial x} \to \frac{\partial}{\partial \zeta} - \frac{1}{c_0}\frac{\partial}{\partial \tau} \quad ; \quad \frac{\partial}{\partial \zeta} \ll \frac{\partial}{\partial \tau}$$

$$t \to \tau = t - \frac{x}{c_0} \quad ; \quad \frac{\partial}{\partial t} \to \frac{\partial}{\partial \tau}$$

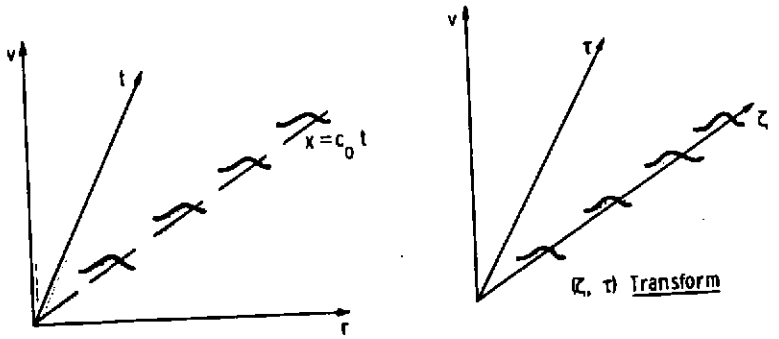

Fig. 3

than the rate-of-change of the waveform with respect to the temporal variable. Thus the result of applying the transformation, which in the form shown is applicable when the waveform is specified as a function of time at some point in space, is that Burger's equation can be very quickly derived and is shown in Fig. 4 where ζ has been rewritten as r for convenience. In deriving Burger's equation from the general second-order-nonlinear wave equation therefore, we have introduced the following restrictions:

1. A one dimensional equation.
2. Progressive waves in one direction only.

However, in return for these restrictions, we have gained a considerable simplification in the form of the wave equation, and this is the primary justification for deriving Burger's equation, i.e., it is an approximate equation which has an extremely simple form, but which nevertheless describes the physics of finite-amplitude wave propagation (to second order) very faithfully.

A further simplification is achieved by introducing the stretched coordinate system derived by Blackstock[9] in order to represent the equation in a nondimensional form which is invariant for signals which, are or are not, subject to spreading losses. This coordinate system is shown in Fig. 5 where, very briefly, the index ℓ defines the type of spreading loss, f is a non dimensional range parameter and y is a dimensionless retarded time. The parameter Γ_o is the plane-wave Acoustic Reynolds number which represents the ratio of nonlinear forces to dissipative forces. As you can see, the numerator is the product of the nonlinear parameter $\beta = (1 + B/2A)$ and the Mach number at the source, ε_o which represent the nonlinearities due to the equation-of-state and the equation-of-motion respectively; whereas the terms in the denominator

Dwg. 2942A83

$$\underline{\text{Burger's Equation}}: - \frac{\partial v}{\partial r} - \left(\frac{\beta}{2C_o^2}\right) \frac{\partial v^2}{\partial \tau} - \left[(2\eta + \eta')/2\rho_o C_o^3\right] \frac{\partial^2 v}{\partial \tau^2} = 0$$

$$\beta = 1 + \frac{B}{2A}; \; r = \zeta$$

Restrictions: – 1.) One Dimensional Wave Motion

2.) Progessive Waves in One Direction

Fig. 4

Dwg. 2942A84

Spreading Loss	ℓ	f/σ_0	$\Gamma(f)$
None	0	r/r_0	Γ_0
Cylindrical	$\frac{1}{2}$	$2\left[(r/r_0)^{\frac{1}{2}} - 1\right]$	$\Gamma_0 \left(1 + \frac{f}{2\sigma_0}\right)^{-1}$
Spherical	1	$\mathrm{Ln}\,(r/r_0)$	$\Gamma_0 \exp(-f/\sigma_0)$

$\sigma_0 = \beta \epsilon_0 r_0/r_L$; $\Gamma_0 = \beta \epsilon_0/\alpha_0 r_L$; $y = (c_0/r_L)\,(t - \frac{r}{c_0})$

Fig. 5

are α_o, the attenuation coefficient at a characteristic source frequency, and r_L, a characteristic length associated with the particular source waveform. In the case of a CW source the characteristic length r_L is chosen as the inverse of the source wavenumber. For signals subject to spreading losses the plane-wave Acoustic Reynolds number is modified as shown in the Table (Fig. 5).

In terms of this notation therefore, Burger's equation takes the form shown in Fig. 6, where capital V is now dimensionless, and the only additional restriction, over and above those already mentioned, is that for signals undergoing cylindrical or spherical spreading loss, we require that $(r/r_L) > 1$. Now the plane wave form of this non-dimensional equation is shown in Fig. 7, where σ represents the dimensionless range parameter in this instance. As shown by Mendousse [2] and discussed by Beyer[1] this equation can be reduced to the form of the linear heat conduction equation by means of the Hopf[15], Cole[16] transformation shown in Fig. 7. Thus, an exact analytical solution of the form shown here can be derived, but as will be mentioned later on, this solution is only peripherally useful, and in the above form it is restricted to CW signals. Although solutions can be obtained in this manner for more general source waveforms, they become increasingly cumbersome to evaluate.

Turning now to the exact analytical solutions which have been derived to-date, we state at the outset that with one exception these are only available for CW signals. To begin with therefore, we consider the solutions of the lossless equation which are obtained by setting the Acoustic Reynolds number equal to infinity. Now in a lossless medium we know from physical considerations that a plane-plane wave of finite-amplitude at the source must become

Dwg. 2942A73

DIMENSIONLESS BURGER'S EQUATION:-

$$\frac{\partial V}{\partial f} - V\frac{\partial V}{\partial y} - \Gamma^{-1}(f)\,\frac{\partial^2 V}{\partial y^2} = 0$$

$$V(r, y) = (r/r_0)^{\ell}\, v(r, y)/v_0 \quad ; \ell = 0, \tfrac{1}{2}, 1$$

Fig. 6

Dwg. 2942A80

PLANE WAVE FORM OF BURGER'S EQUATION:-

$$\frac{\partial V}{\partial \sigma} - V\frac{\partial V}{\partial y} - \Gamma_o^{-1}\frac{\partial^2 V}{\partial y^2} = 0$$

Hopf - Cole Transformation:- $V = \frac{2}{\Gamma_o}\left[\text{Ln } \varepsilon\right]_y$

$$\frac{\partial \varepsilon}{\partial \sigma} - \Gamma_o^{-1}\frac{\partial^2 \varepsilon}{\partial y^2} = 0$$

Solution:- $$V = \frac{2}{\Gamma_o}\frac{\partial}{\partial y}\,\text{Ln}\left\{\sum_{n=o}^{\infty} \varepsilon_n (-1)^n I_n(\Gamma_o/2) e^{-n^2\sigma/\Gamma_o}\cos ny\right\}$$

Fig. 7

increasingly distorted as it propagates through the medium until eventually enough harmonics are generated and shock formation occurs. We can therefore consider the propagation history of such a signal to consist of two zones, I and II, where Zone I exists from the source to the point at which shock formation occurs, and Zone II is the domain where the waveform has a sawtooth profile. The lossless Zone I solutions are shown in Fig. 8, where as previously stated the signal is CW. The time waveform has the classical Riemann form[17] with the function invariantly imbedded in the argument. By making a harmonic analysis of this solution Hargrove[18] obtained the Fubini spectral distribution[19] or as Blackstock has called it, the "Bessel-Fubini solution".

Since this solution is that of a continually distorting waveform we can readily find its range of validity, i.e., the extent of Zone I, by determining the range at which the derivative with respect to y (which is the dimensionless retarded time) approaches infinity - this occurs when the dimensionless range parameter f is equal to unity. We can thus determine the dimensional range at which shock formation occurs as a function of the source frequency and Mach number from the conversion table of Fig. 5.

Another method for obtaining the lossless Zone I solution, due to Banta[20], is shown in Fig. 9 where the normalized particle velocity is expressed as a Taylor series, and D_f^s is the s^{th} derivative with respect to f. As Banta[20] has shown, this can be reduced to an elegant operational form outlined in Fig. 9, by means of which the Bessel-Fubini solution can be derived for a CW signal. Using this operational solution the author was able to obtain the lossless Zone I parametric spectrum for a source waveform with two frequency components[21] which is shown in Fig. 10. The parametric

Dwg. 2945A29

LOSSLESS ZONE I SOLUTIONS: -

Riemann: - $V = V(y + f V)$

Fubini: - $= \sum_{n=1}^{\infty} \frac{2}{nf} J_n(nf) \sin ny;$ for $V(o, y) = \sin y$

Critical: - $\frac{\partial v}{\partial y} \to \infty$

$f_c = 1$

Fig. 8

[illegible] SOLUTIONS (Continued) :-

Series: $V(f,y) = \sum_{n=0}^{\infty} \frac{f^s}{s!} D_f^s V(o,y)$; $D_f^s = \frac{d^s}{df^s}$

$$= \left\{ \exp\left\{ f D_f V(o,y) \right\} - 1 \right\} / f D_f$$

[illegible] $V(o,y) = \sin(y)$

Then $V(f,y) = \sum_{n=1}^{\infty} \frac{2}{nf} J_n(nf) \sin ny$

Fig. 9

When $V(o, y) = V_{01} \sin(N_1 y) + V_{02} \sin(N_2 y)$; $\qquad N_i = \omega_i/(\omega_1 - \omega_2)$, integer; $i = 1, 2$

Then $$V(f, y) = \sum_{n=0}^{\infty} \sum_{m=0}^{\infty} \frac{2(\pm 1)^m}{(n N_1 \pm m N_2) f} J_n\left[(n N_1 \pm m N_2) f V_{01}\right] J_m\left[(n N_1 \pm m N_2) f V_{02}\right] \sin(n N_1 \pm m N_2) y$$

Time Waveform: - $V = V_{01} \sin N_1 (y + f V) + V_{02} \sin N_2 (y + f V)$

Dimensionless Critical Range: - $f_c = 1/(V_{01} N_1 + V_{02} N_2)$

Dimensional Critical Range: - $r_c = 1/\beta (\epsilon_{01} k_{01} + \epsilon_{02} k_{02})$

Fig. 10

time-waveform solution is also shown together with the dimensionless critical range and its dimensional counterpart. It should be noted that for small values of V_{01} and V_{02} the spectral representation for the plane wave case can be reduced to the form of an approximate solution derived by Naugolnykh, Soluyan and Khokhlov.[6]

So much for the lossless Zone I solutions. In Fig. 11 we see the lossless Zone II solution derived by Naugolnykh[4], Westervelt[2], and Blackstock,[9] where V_{po} represents the normalized peak amplitude at the spreading distance, r_o. Essentially, this solution is readily obtained from physical considerations since we know that the waveform in this zone has a periodic sawtooth form, $A(\pi-y)$ between $-\pi$ and π, (where A is a parameter which depends on f), and thus by substituting this solution in the lossless form of Burger's equation the parameter A is easily derived, so that the solution has the form shown. An asymptotic relationship between the lossless Zone I and II solutions obtained by Blackstock[10] is shown in Fig. 12, for the fundamental harmonic component, B_1. Having obtained the lossless solution for Zones I and II, we can very quickly obtain the much more interesting Zone II solution for a viscous medium, by means of an asymptotic technique used by Naugolnykh, Soluyan and Khokhlov[5] in their analysis of spherically spreading finite-amplitude waves. This is shown in Fig. 13 where the derivation is as follows: Let us assume the existence of a wave of permanent profile, i.e., a wave which is independent of variations in the spatial derivatives. If such a wave exists, its functional form can be determined by equating the spatial-derivative in Burger's equation to zero and then solving the equation thus formed. The solution of this reduced equation, known as the "dynamic-steady-state" (d.s.s.) solution has the form shown,

$$= [\alpha_0 \alpha_1 \alpha_2]$$

Curve 641865-A

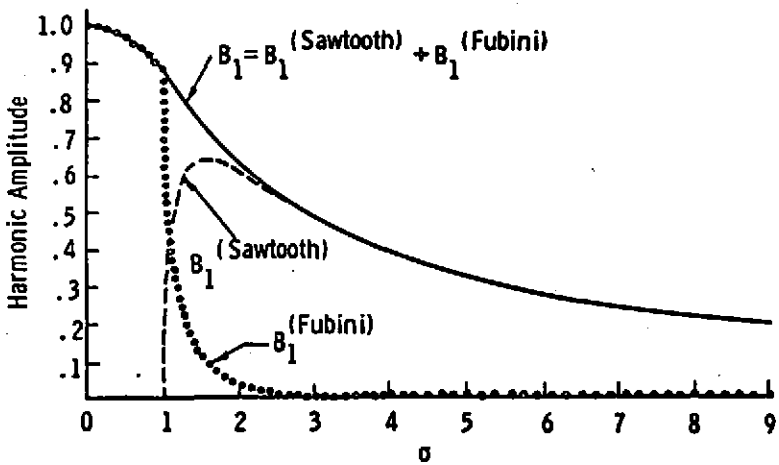

Fig. 12

Dwg. 2942A74

SINGLE SINE WAVE VISCOUS D.S.S. SOLUTION (Zone II)

$$\text{If } \frac{\partial V}{\partial f} \to 0 \text{ Then } V\frac{\partial V}{\partial y} - \Gamma^{-1}(f)\,\frac{\partial^2 V}{\partial y^2} = 0$$

Solution:- $V = C(f)\tanh\left[C(f)\Gamma(f)\,y/2\right]$

$\to C(f) = \pi/(1+f)$

$\Gamma \to \infty$

$y \to 0$

Hence $$V = \frac{1}{1+f}\left[-y + \pi\tanh\left(\frac{\pi\Gamma(f)\,y}{2(1+f)}\right)\right]$$; Soluyan & Khokhlov

$$= \frac{2}{\Gamma(f)}\sum_{n=0}^{\infty}\frac{\sin n y}{\sinh\left[n(1+f)/\Gamma(f)\right]}$$; Fay

Fig. 13

where C is an undetermined parameter, and of course Γ is the Acoustic Reynolds number, which as previously mentioned is the ratio of nonlinear forces to dissipative forces. If the medium was lossless this d.s.s. solution would have to relax asymptotically to the lossless Zone II solution which we have just considered. Thus by equating Γ to infinity (i.e. zero viscosity) and y equal to zero we find that the d.s.s. solution is reduced to the constant C which in turn must be equal to the lossless Zone II solution at $y = 0$, which is $\pi/(1+f)$. Thus C has been determined, and by adding an additional term $- y/(1+f)$ to the d.s.s. solution we obtain the exact particular solution of Burger's equation, shown in Fig. 13, which was first derived by Soluyan and Khokhlov.[3] Soluyan and Khokhlov[3] originally obtained this solution by applying the method of stationary phase to the integral solution of the heat conduction equation obtained by means of the Hopf-Cole transformation previously discussed. Making a harmonic analysis of the Soluyan & Khokhlov,[3] solution we thus obtain the spectrum derived independently by Fay[23] in 1931, which is valid for $\Gamma_o >> 1$. Before considering the conditions for the existence of this viscous Zone II solution we can summarize the sequence of contributions which have been discussed, as shown in Fig. 14, where you can see that the Soluyan and Khokhlov time-waveform solution can be derived from the d.s.s. solution via the asymptotic matching procedure, just discussed, or via the asymptotic integral evaluation employed by Soluyan and Khokhlov themselves. A Fourier analysis of this solution thus gives the Fay spectrum. Alternately, since the Fay spectrum can also be derived from the linear heat conduction equation, as shown by Blackstock[11] we can then make an inverse Fourier analysis of this spectrum and obtain the Soluyan and

Dwg. 2942A96

Single Sine Wave
Viscous Zone II Solution:- $V(f, y) = -\left\{y + \pi \tanh\left[y/\Delta(f)\right]\right\} / (1+f)$

$$= \frac{2}{\Gamma(f)} \sum_{n=0}^{\infty} \frac{\sin ny}{\sinh\left[n(1+f)/\Gamma(f)\right]}$$

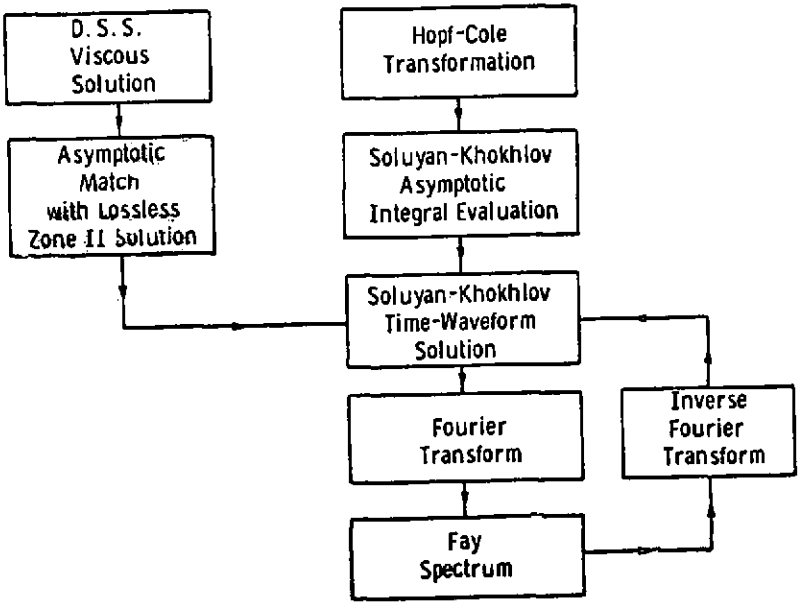

Fig. 14

Khokhlov time waveform. A comparison of the lossless and viscous Zone II waveforms is shown in Fig. 15, where it is clear that the effect of dissipation is simply to round off the corners of the waveform thus causing the shock front to have a finite thickness S_T. Now the shock thickness S_T can be derived from the Soloyan and Khokhlov solution, and since it must be less than one period of the waveform, Blackstock[11] arbitrarily defined the upper limit of S_T to be $\sim 2\pi/5$, i.e., if S_T exceeds this value then the Zone II solution is inapplicable. This is shown in Fig. 16 and consequently, according to Blackstock[11] and Cary[26] the Acoustic Reynolds number must satisfy the inequality outlined below. We can thus determine the extent of Zone II, if it exists, by calculating the value of the dimensionless range f_s which just satisfies the equality. For values of f greater than f_s the inequality is violated. Likewise, since we know from the lossless Zone I solution for a CW signal that the onset of Zone II occurs when the dimensionless range parameter f is equal to unity we can thus select a somewhat larger value of f such as $\pi/2$ to determine the onset of Zone II in a dissipative medium - a choice which Blackstock found was compatible with a numerical analysis of the exact solution of Burger's equation derived by Mendousse,[2] which we previously discussed. Inserting this value of f in the inequality therefore,

Cary[24] obtained a criterion for the onset of shock formation (or the existence of Zone II) which is one of the most useful results obtained from the solution of Burger's equation. This criterion, expressed in terms of dimensional parameters, is shown in Fig. 17, and in this form we can use it to predict the source sound pressure level which will cause shock formation to occur for a CW source of given frequency and aperture dimensions. This result of the theory

Dwg. 2942A99

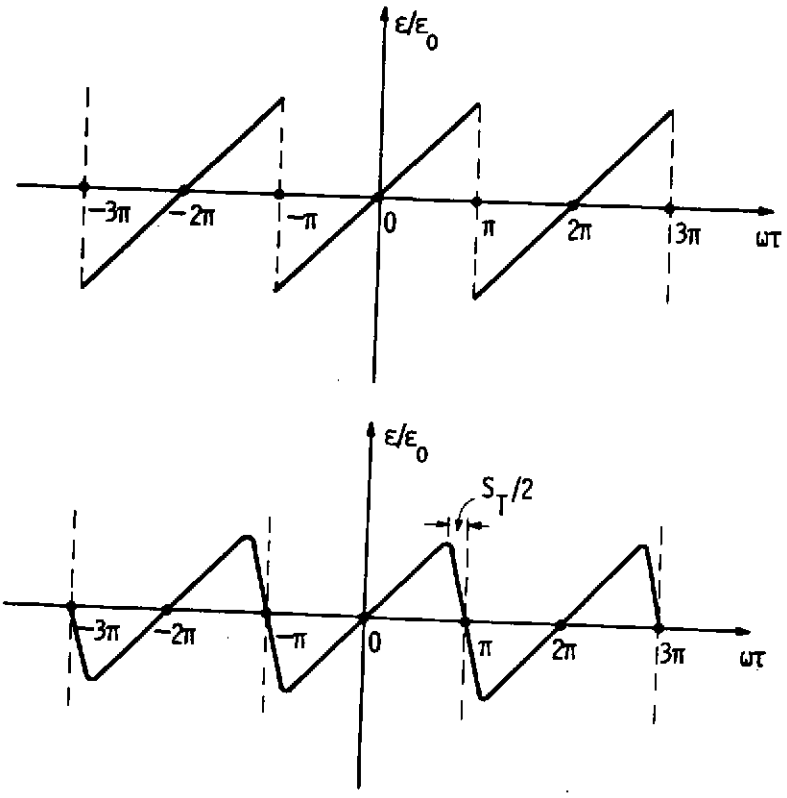

Fig. 15

Dwg. 2942A87

If $S_T \leq 2\pi/5$ then $\Delta_{max} = \pi/8.7$

and $\Gamma(f) \geq (17.4/\pi^2)(1+f)$, $\pi/2 \leq f \leq f_s$

Thus $\Gamma(f_s) = (17.4/\pi^2)(1+f_s)$

and $\Gamma(\pi/2) \geq (17.4/\pi^2)(1+\pi/2)$

Fig. 16

Dwg. 2942A82

CRITERION FOR SHOCK FORMATION:-

$$r_0 \geq (4.5)\left[r_c^{(\ell)}/r_0\right]^{\ell},\ \ell = 0,\ 1/2,\ 1$$

$$r_c^{(0)}/r_0 = (\pi/2\,\beta\epsilon_0)\,(r_L/r_0)$$

$$r_c^{(1/2)}/r_0 = \left\{1 + 1/2\,(r_c^{(0)}/r_0)\right\}^2$$

$$r_c^{(1)}/r_0 = \exp\left[r_c^{(0)}/r_0\right]$$

Fig. 17

has been discussed by Smith and Berktay[25] I believe, and in Fig. 18 we see the criterion represented graphically for signals subject to spherical spreading loss in the form of curves of SPL at the Rayleigh distance vs frequency for three different source diameters. These curves were computed for fresh water with the small signal attenuation coefficient shown. Points above these curves correspond to sound pressure levels and frequencies sufficient to cause the occurrence of shock formation beyond the Rayleigh distance for the particular source frequencies and diameters considered. Points on the curves represent threshold values, and points below the curves represent values of SPL and frequency which are not sufficient to cause the onset of shock formation beyond the spreading distance. Of course plane wave shock formation may occur within the spreading distance for a particular CW source and the possibility of this occurrence can be determined by examining the ratio of the critical range at which shock formation occurs to the spreading distance - evaluated as a function of source diameter and frequency. This ratio of critical range to spreading distance for a CW source in fresh water is shown in Fig. 19, and it is clear that if the ratio exceeds unity then shock formation can only occur beyond the Rayleigh distance for the particular frequencies and source diameters under consideration. Another useful result of the analytical expressions which we have just considered is that they can be used to predict the amount of finite-amplitude attenuation suffered by a CW signal in generating a harmonic spectrum during its course of propagation through the medium. This has been discussed in detail by Blackstock[11], Cary[26] and by Smith and Berktay[25] so that we can pass on to the next topic which is concerned with the numerical solution of Burger's equation. Summarizing what has been

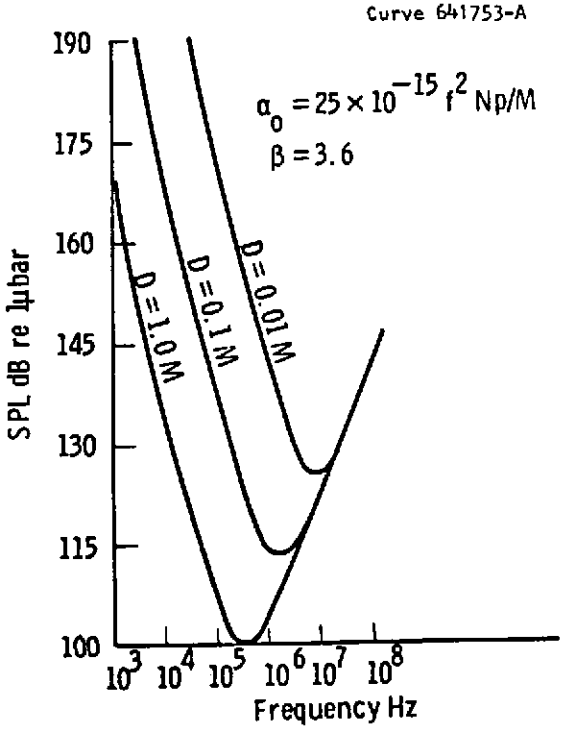
Curve 641753-A
190
175
160
145
130
115
100
SPL dB re μbar
$\alpha_0 = 25 \times 10^{-15} f^2$ Np/M
$\beta = 3.6$
D = 1.0 M
D = 0.1 M
D = 0.01 M
10^3 10^4 10^5 10^6 10^7 10^8
Frequency Hz

Fig. 18

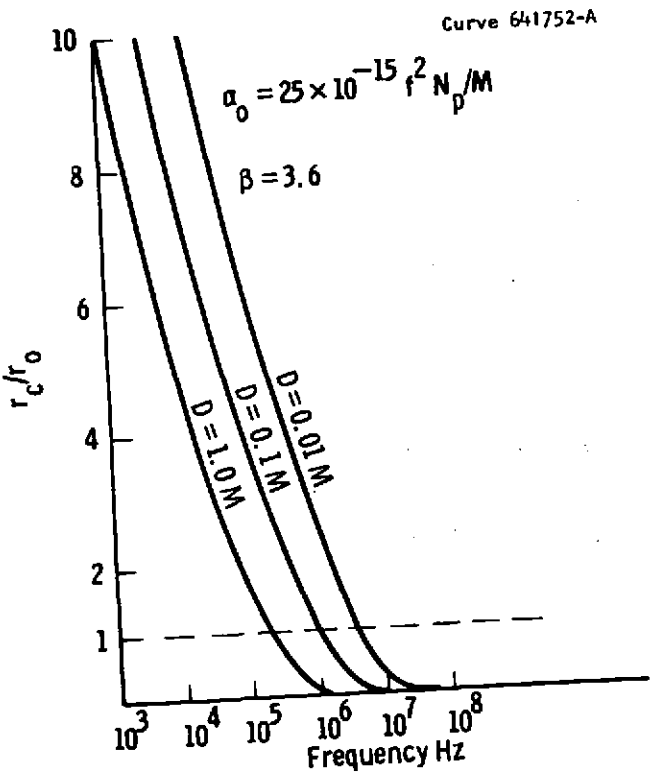
Curve 641752-A
$\alpha_0 = 25 \times 10^{-15} f^2 N_p/M$
$\beta = 3.6$
D=0.01 M
D=0.1 M
D=1.0 M
r_c/r_o
10
8
6
4
2
1
10^3
10^4
10^5
10^6
10^7
10^8
Frequency Hz

Fig. 19

accomplished analytically therefore, we have seen that exact Zone I solutions of the lossless Burger's equation are available for CW signals and for more general waveforms. However, Zone II solutions have only been obtained for CW signals.

Even if such solutions are obtained they will still have to be supplemented by numerical analysis for the case of completely arbitrary source waveforms. I should mention at this point that Naugolnykh, Soluyan and Khokhlov[6] and independently the author[27] have applied the method of successive approximations to obtain approximate solutions of Burger's equation for the case of parametric interactions between CW signals and the self interaction of amplitude modulated waves. Some of these solutions will be briefly referred to later on in this talk. Thus, passing on to Fig. 20 we have an encapsulated summary of the numerical methods applied to Burger's equation prior to 1970.

The first numerical solution of note is due to Blackstock[11] who made a numerical harmonic analysis of the Hopf-Cole-Mendousse[2] exact plane-wave-solution for CW signals, which we previously discussed, in order to evaluate the spectral amplitudes as a function of range. This analysis was performed with increasing values of the Acoustic Reynolds number Γ_o, and as Blackstock discovered, the numerical accuracy seriously deteriorated for values of Γ_o greater than fifty. This was primarily due to the slow convergence and alternating signs of the terms of the Bessel-Function series in the numerator and denominator of the quotient (see Fig. 7). Consequently, harmonic analysis of exact solutions of this form cannot be recommended, particularly as they become increasingly complicated when the source waveform contains more than one frequency component.

NUMERICAL METHODS: -

1. Harmonic Analysis of the Hopf-Cole-Mendousse Exact Plane-Wave Solution (Blackstock);
   Fails when $\Gamma_0 > 50$
2. Finite-Difference Mesh (Marsh-Mellen-Konrad)
3. Taylor Series Expansion (Banta-Cary)

$$V(f_i, y) = \sum_{s=0}^{\infty} \frac{(\Delta f)^s}{s!} \left[D_f^s V(f_{i-1}, y) \right] \; ; \; f_{i-1} + \Delta f = f_i \; ; \; i = 1, 2, \ldots$$

$$\left[D_f V \right] = V \left[D_y V \right] + \Gamma^{-1}(f) \left[D_y^2 V \right]$$

$$\left[D_f^2 V \right] = \left[D_f V \right] \left[D_y V \right] + V D_y \left[D_f V \right] + \left[D_f \Gamma^{-1}(f) \right] \left[D_y^2 V \right] + \Gamma^{-1}(f) D_y^2 \left[D_f V \right]$$

Fig. 20

The next application of numerical methods to a more general form of Burger's equation which included dispersive terms, was carried out by Marsh, Mellen, and Konrad[28] who used a finite-difference mesh to replace the equation by a set of linear algebraic equations which were then solved on a digital computer by standard Matrix procedures.

In order to decrease the computation time required to obtain solutions via finite-difference approximations, Cary[24] extended the technique which had been applied by Banta to the solution of the lossless Burger's equation, which we considered earlier on. This method, originally due to Lagrange, consists in expanding the normalized particle velocity in a Taylor series as shown, and then obtaining analytical expressions for the derivatives which appear in this series via the differential equation. I should point out that f_i (subscript i) represents the value of f at the ith field point and the increment Δf in the Taylor series represents the dimensionless spatial distance between two field points. Once again D_f^s represents the sth derivative with respect to f, and in this notation Burger's equation has been reexpressed as shown. Looking at the equation in this form it is immediately evident that the first derivative with respect to f which appears in the Taylor series is given by Burger's equation itself in terms of derivatives of V with respect to y. Thus, if we are given the waveform as a function of time at some point in space, which could, but need not be, the source itself, we can compute the first derivative with respect to f at this point by differentiating the waveform with respect to y the required number of times and inserting these derivatives in the terms on the right hand side of the equation. In order to obtain algebraic relationships for the higher derivatives with respect to f in terms of derivatives with respect to y, which we can compute, we differentiate Burger's equation with

respect to f and replace all terms on the right-hand-side which contain the first derivative with respect to f with the right-hand-side of the previous equation. In this manner the second derivative with respect to V is obtained in terms of derivatives with respect to y. Continuing in this manner the higher derivatives with respect to f can be expressed recursively in terms of derivatives with respect to y, although the degree of complexity increases with each successive f derivative, making it impractical to go beyond the sixth order. However, the advantage gained in using more than three derivatives in the Taylor series is that it permits larger increments in Δf to be used, than would be required for convergence with a finite-difference mesh, which only makes use of the first two terms in the Taylor series as the basis for approximating the derivatives. Once expressions for the f derivatives have been obtained therefore, in terms of y derivatives, they can be readily programmed, and once the time waveform has been specified at some field-point all of the subsequent calculations can easily be carried out on a digital computer. Thus, if we are only interested in computing the time waveform of a finite-amplitude signal as it propagates through the medium this method can be very useful. It can also be readily extended to the case of a dispersive medium as shown by Cary and Fenlon.[29] The method does have its disadvantages however, especially if one is primarily interested in computing the spectral levels of the nonlinearly generated harmonics as the signal propagates through the medium. These disadvantages are related to the required numerical operations which are briefly summarized in Fig. 21.

As an alternative to this method, the author[27] found it preferable to express the normalized particle velocity as a Fourier

Dwg. 2927A62

NUMERICAL OPERATIONS REQUIRED

1. Source Waveform Sampled at the Nyquist Rate
2. Filter to Remove Spurious Harmonics Above the cut - off Frequency
3. Numerical Differentiation
4. Numerical Harmonic Analysis

Fig. 21

series, shown in Fig. 22, which enables Burger's equation to be replaced by a coupled set of ordinary nonlinear differential equations with the spectral amplitudes as the dependent variables. In this set of equations the spectral amplitudes are complex, and the term $\tilde{V}_n * \tilde{V}_n$ represents the self-convolution of the signal in frequency space. Since the solution of these coupled equations have been discussed elsewhere[27] the method-of-solution is only very briefly outlined in Fig. 23. Here we see the coupled-modal form of Burger's equation written out again, and below it we see the spectral amplitudes expressed as a Taylor series, where the matrix $C^a_{n,i}$ represents the f derivatives as shown. Using the same technique applied in the Banta-Cary method we can thus obtain an expression for the n^{th} derivative with respect to f in terms of the $(n-1)^{th}$ derivative, which in this instance results in the general recurrence relationship shown below. I might just add that it is preferable to use a Taylor series expansion rather than a power series to represent the spectral amplitudes when the Acoustic Reynolds number is a function of f (as it is when we have cylindrical or spherical spreading) because it turns out that in this instance we can take repeated derivatives of Γ^{-1} (f) with respect to f rather than having to represent Γ^{-1} (f) as a power series which would otherwise be required. The advantages of the recurrence technique are summarized in Fig. 24.

A further development of this technique for computing the transient response of signals can now be readily implemented. Thus, in Fig. 25 we see, for simplicity, the unnormalized plane-wave form of Burger's equation in terms of the dimensional variables v, r, and τ, and below it we see the particle velocity expressed as the inverse Fourier transform of its spectrum. When the latter is inserted in Burger's equation therefore, we obtain an equation for the spectral

Dwg. 2942A81

(4) SPECTRAL REDUCTION OF BURGER'S EQUATION (FHF)

$$V(f,y) = \sum_{n=-\infty}^{\infty} \tilde{V}_n(f) \exp(jny)$$

$$\frac{d\tilde{V}_n}{df} + n^2 \Gamma^{-1}(f)\, \tilde{V}_n - (jn/2)\, \tilde{V}_n \circ \tilde{V}_n = 0$$

$$\tilde{V}_n \circ \tilde{V}_n = \sum_{n=-\infty}^{\infty} \tilde{V}_{n-m}(f)\, \tilde{V}_m(f)$$

$$= 1/2 \sum_{m=1}^{n-1} \tilde{V}_{n-m}(f)\, \tilde{V}_m(f) - \sum_{m=1}^{\infty} \tilde{V}_{n+m}(f)\, \tilde{V}_m(f)$$

Fig. 22

Dwg. 2942A86

$$\frac{d\tilde{V}_n}{df} + n^2 \Gamma^{-1}(f)\, \tilde{V}_n - (jn/2)\, \tilde{V}_n \circ \tilde{V}_n = 0$$

$$\tilde{V}_n(f_{i+1},\, y) = \sum_{s=0}^{S} C^s_{n,i} (\Delta f)^s;\quad f_{i+1} = f_i + \Delta f$$

$$C^s_{n,i} = (1/s!)\, D_f^s \tilde{V}_n(f_i)$$

$$C^{s+1}_{n,i} = -\sum_{q=0}^{s} \left[(n^2/q!) \left\{ D_f^q \Gamma^{-1}(f_i)\, C^{s-q}_{n,i} \right\} - (jn/2) \sum_{m=-\infty}^{\infty} C^{s-q}_{n-m,i}\, C^q_{m,i} \right] / (s+1)$$

Fig. 23

Dwg. 2927A63

ADVANTAGES OF THE RECURRENCE RELATIONSHIP

1. Periodic Source Waveforms with $V(f_0, -\tau) = -V(f_0, \tau)$

- Eliminates Waveform Sampling
- Eliminates Filtering the Source Waveform
- Eliminates Numerical Differentiation
- Eliminates Numerical Harmonic Analysis

2. Arbitrary Source Waveforms of Finite Duration in the τDomain

- Eliminates Numerical Differentiation
- Eliminates Numerical Spectral Analysis

Fig. 24

Dwg. 2942A78

TRANSIENT ANALYSIS:-

$$\frac{\partial v}{\partial r} - (\beta/c_0^2)\, v \frac{\partial v}{\partial \tau} - \left(\frac{2\eta + \eta'}{2\rho_0 c_0^3}\right) \frac{\partial^2 v}{\partial \tau^2} = 0 \qquad ; \tau = t - \frac{r}{c_0}$$

$$v(r,\tau) = \int_{-\infty}^{\infty} \tilde{v}(r,\omega)\, e^{j\omega\tau}\, d\omega/2\pi$$

$$\frac{d\tilde{v}}{dr} + \alpha_0(\omega)\, \tilde{v} - (j\beta\omega/2c_0^2)\, \tilde{v} \circ \tilde{v} = 0 \qquad ; \alpha_0(\omega) = (2\eta + \eta')\, \omega^2/2\rho_0 c_0^3$$

$$\tilde{v} \circ \tilde{v} = \int_{-\infty}^{\infty} \tilde{v}(r,\omega')\, \tilde{v}(r,\omega-\omega')\, d\omega'/2\pi$$

$$\equiv \int_{-\infty}^{\infty} v^2(r,\tau)\, e^{-j\omega\tau}\, d\tau = F\left\{v^2(r,\tau)\right\}$$

Fig. 25

amplitudes, which as before, includes the self-convolution of the signal. But since the latter is equal to the Fourier Transform of the signal squared, it is immediately obvious that we can make use of the powerful machinery of digital signal processing which utilizes the Fast Fourier Transform (F.F.T.) algorithm to rapidly switch from the time waveform to the spectrum as the solution is obtained at each incremental distance from the source. In order to use the F.F.T. it is of course necessary to sample the spectrum at a rate which depends upon the number of significant spectral components generated during the course of propagation through the medium. Usually this can be estimated from experience and a consistency check can be readily made using a different sampling rate. Now you will notice that the coupled modal form of Burger's equation enables us to immediately express the finite-amplitude attenuation coefficient, in terms of its small signal value together with an additional term which is the self-convolution of the signal divided by the spectral vector. Thus, when all the significant spectral components have been formed by means of the recurrence relationship, this expression for the finite-amplitude attenuation coefficient, which is shown in Fig. 2b, can be used to compute the spectrum at all subsequent values of range. In general, this method requires the use of a smaller spatial increment Δf, which implies a slower rate-of-convergence. On the other hand, since it only requires the evaluation of a single summation (integral) compared with the double summation which appears in the recurrence relationship, the computation time required is considerably reduced. Note that in the last few diagrams the equations have been shown in dimensional form, and only for the plane wave case. This was done merely to simplify the presentation, since Blackstock's stretched coordinate system must be modified slightly when we are dealing with the transient response of finite-amplitude signals. I wish to emphasize this point because when performing numerical calculations

Dwg. 2942A70

FINITE-AMPLITUDE ATTENUATION COEFFICIENT :-

$$\alpha_F(r,\omega) \triangleq -\frac{1}{\tilde{v}}\frac{d\tilde{v}}{dr}$$

$$= \alpha_0(\omega) + (j\beta\omega/2c_0^2)\int_{-\infty}^{\infty}\left[\tilde{v}(r,\omega')\,\tilde{v}(r,\omega-\omega')/\tilde{v}(r,\omega)\right]d\omega'/2\pi$$

Fig. 26

it is preferable to work with the equations in nondimensional form. As an example of the use of the numerical computational procedure Fig. 27 shows a calculation of the normalized fundamental component of a plane CW signal plotted as a function of normalized range for increasing values of the Acoustic Reynolds number. These calculations were made to check the accuracy of the procedure by comparison with a similar set of curves computed by Cook.[30] Cook's[30] numerical technique I might add is not based on the use of Burger's equation and depends on a phenomenological representation of the term which on the previous slide we identified as the self-convolution of the signal in frequency space. Thus, although Cook's[30] method appears to give useful results for plane CW signals it is not clear how it can be extended to deal with more general waveforms. The computed results shown in this slide agree to within graphical accuracy with Cook's results, and as you can see the result of finite-amplitude attenuation is that source saturation occurs as the Acoustic Reynolds number increases - which is consistent with the plane-wave finite-amplitude results obtained by Blackstock[11]. Fig. 28 shows the variation of second harmonic levels relative to the fundamental as a function of range, for the same values of the Acoustic Reynolds number. Once again, these computed results agree with those of Cook to within graphical accuracy and the same is true of the higher harmonic components. Of course, I wish to emphasize again that this is only an example which was used to check the accuracy of the computational procedure. This procedure then, is outlined schematically in the form of a block diagram in Fig. 29 which is self-explanatory. Thus with the use of the F.F.T. algorithm the transient response of arbitrary source waveforms such as coded pulses can readily be evaluated as a function of distance from the source. Finally, I would like to

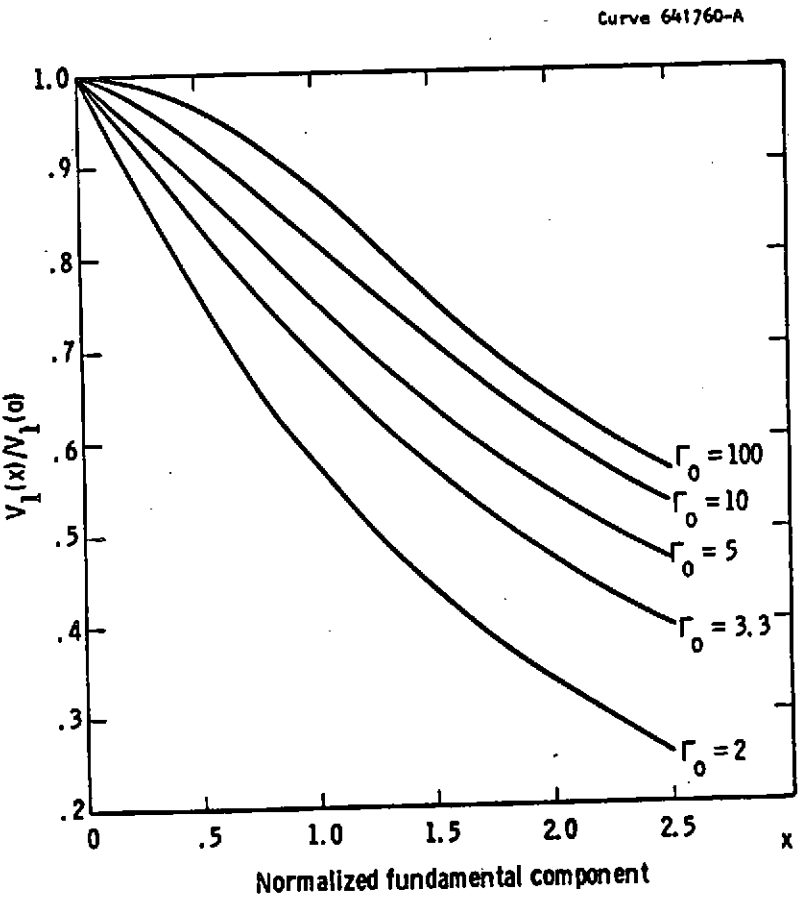
Curve 641760-A
1.0
.9
.8
.7
.6
.5
.4
.3
.2
$V_1(x)/V_1(o)$
$\Gamma_0 = 100$
$\Gamma_0 = 10$
$\Gamma_0 = 5$
$\Gamma_0 = 3.3$
$\Gamma_0 = 2$
0
.5
1.0
1.5
2.0
2.5
x
Normalized fundamental component

Fig. 27

Curve 641759-A

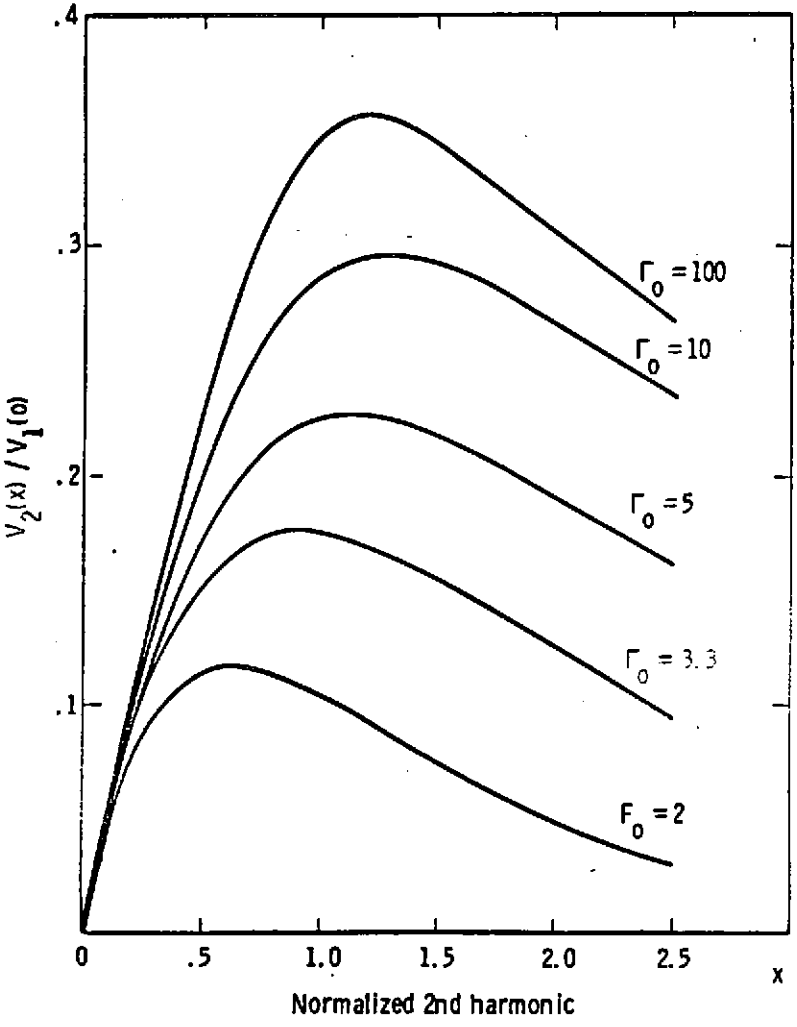

Fig. 28

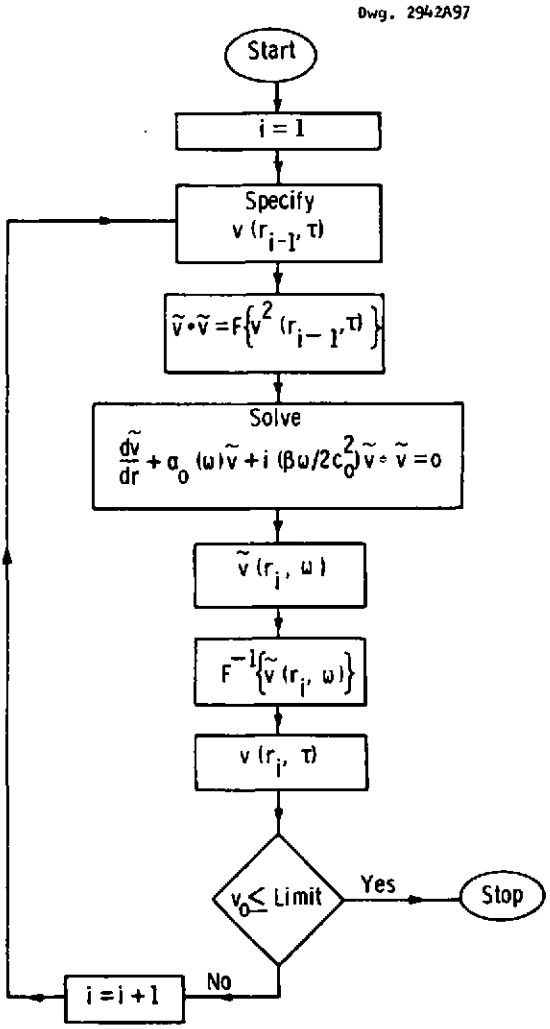
Dwg. 2942A97
Start
i = 1
Specify
v (r_{i-1}, τ)
F{v^2 (r_{i-1}, τ)}
Solve
dṽ/dr + α_0 (ω) ṽ + i (βω/2c_0^2) ṽ · ṽ = 0
ṽ (r_i, ω)
F^{-1}{ṽ (r_i, ω)}
v (r_i, τ)
v_0 ≤ Limit
Yes
Stop
No
i = i + 1

Fig. 29

discuss the transient solution obtained by applying the method-of-successive-approximations to the coupled-modal form of Burger's equation. This is shown in Fig. 30 where spreading losses have been excluded to simplify the presentation. Now the first-order-approximation is obtained by neglecting the self-convolution term, and the second-order-approximation is then obtained by substituting the first-order-approximation in the self-convolution term as shown and then solving the resulting equation to give the solution outlined below.

If we consider the case of parametric interaction between two CW pulses of finite-amplitude, and neglect the influence of all other spectral components on the difference-frequency pulse spectrum - a simplification which is consistent with the accuracy of the second-order-approximation - we can obtain the far field transient response for the difference-frequency signal as shown in Fig. 31 which is identical to that derived by Muir and Blue.[31] And in Fig. 32 we see the same spectrum when the effect of spreading loss is included for the parametrically generated difference-frequency signal, where the spreading distance r_{od} is represented by the Rayleigh distance which is given by $k_{od}S_o/4\pi$ for a circular piston in a rigid baffle.
The first term in this solution has the well known functional form originally derived by Westervelt.[32] The solution assumes of course that the primary signals are not subject to spreading, i.e., that parametric interaction takes place within the Fresnel zone of the primary signals.

In conclusion therefore, we have seen that the coupled-modal form of Burger's equation and the resulting expression for the finite-amplitude attenuation coefficient, form the basis of a general procedure for evaluating the spectral interactions of the progressive finite-amplitude signals of arbitrary spectral composition at the

SUCCESSIVE APPROXIMATION (PLANE - WAVE EXAMPLE) :-

$$\frac{d\tilde{V}}{dr} + \alpha_o(\omega)\tilde{V} - (j\beta\omega/2c_o^2)\,\tilde{V}\circ\tilde{V} = 0$$

Hence $\tilde{V}^{(1)}(r,\omega) = \tilde{V}(o,\omega)\,e^{-\alpha_o(\omega)r}$

and $\frac{d\tilde{V}^{(2)}}{dr} + \alpha_o(\omega)\tilde{V}^{(2)} = (j\beta\omega/2c_o^2)\int_{-\infty}^{\infty}\tilde{V}(o,\omega')\,\tilde{V}(o,\omega-\omega')e^{-\{\alpha_o(\omega')+\alpha_o(\omega-\omega')\}r}\,d\omega'/2\pi$

Hence $\tilde{V}^{(2)}(r,\omega) = e^{-\alpha_o(\omega)r}\left[\int_{-\infty}^{\infty}\tilde{V}(o,\omega')\,\tilde{V}(o,\omega-\omega')Q(r,\omega,'\omega)\,d\omega'\right]$

Where $Q(r,\omega'\omega) = \dfrac{\exp\left[-\{\alpha_o(\omega')+\alpha_o(\omega-\omega')\}r\right] - \exp\left[-\alpha_o(\omega)r\right]}{2\pi\left[\alpha_o(\omega')+\alpha_o(\omega-\omega')-\alpha_o(\omega)\right]}$

Fig. 30

If $v(o,\tau) = \{U(t+T) - U(\tau-T)\}\left[V_{01}\cos\omega_1\tau + V_{02}\cos\omega_2\tau\right]$

and $\alpha_{o1}r \gg 1$, $\alpha_{02}r \gg 1$, with $\tilde{v}(o,\omega_d) = 0$

then $\tilde{v}^{(2)}(r,\omega_d) \simeq \dfrac{j\beta\omega_d}{4\pi c_o^2\alpha_T}\left[\int_{-\infty}^{\infty}\tilde{v}(o,\tilde{\omega})\,\tilde{v}(o,\omega_d-\omega')\,d\omega'\right]e^{-\alpha_o(\omega_d)r}$

$$= \frac{\beta\omega_d V_{01}V_{02}}{4\pi c_o^2\alpha_T}e^{-\alpha_o(\omega_d)r}\left[\frac{\sin(\omega_d-\omega_{od})T}{(\omega_d-\omega_{od})} + \frac{\sin(\omega_d+\omega_{od})T}{(\omega_d+\omega_{od})}\right]$$

where $\omega_{od} = (\omega_1-\omega_2)$, and $\alpha_T = \alpha_{01}+\alpha_{02}-\alpha_{0d}$

Fig. 31

INTRODUCING SPREADING LOSS,

$$\tilde{V}(r,\omega_d) = \frac{r_{od}}{r}\left(\frac{\beta\omega_d V_{01}V_{02}}{4\pi c_o^2\alpha_T}\right)\left[\frac{\sin(\omega_d-\omega_{od})T}{(\omega_d-\omega_{od})} + \frac{\sin(\omega_d+\omega_{od})T}{(\omega_d+\omega_{od})}\right]e^{-\alpha_{od}r}$$

$$= \left(\frac{S_o\beta\omega_d^2 V_{01}V_{02}T}{16\pi^2 c_o^3\alpha_T r}\right)\left[\mathrm{sinc}(\omega_d-\omega_{od})T + \mathrm{sinc}(\omega_d+\omega_{od})T\right]e^{-\alpha_{od}r}$$

where $r_{od} = \dfrac{k_d S_o}{4\pi}$, and $S_o = \pi a^2$

Fig. 32

source, as a function of range. And the attractive feature of this procedure is that it can be applied numerically or analytically depending on the degree of complexity involved.

REFERENCES

1. R. T. Beyer, "Physical Acoustics" (Academic Press, New York 1965) pp. 231-263.
2. J. S. Mendousse, J. Acoust. Soc. Am., 25, 51-54 (1953).
3. S. I. Soluyan and R. V. Khokhlov, Vestn. Mosk. Univ. Ser. III Fiz. Aston. 3, 52 (1961).
4. K. A. Naugolnykh, Soviet Physics-Acoustics, 5, 79-84 (1959).
5. K. A. Naugolnykh, S. I. Soluyan and R. V. Khokhlov, Soviet Physics-Acoustics, 9, 42-46 (1963).
6. K. A. Naugolnykh, S. I. Soluyan, and R. V. Khokhlov, Soviet Physics-Acoustics, 9, 155-159 (1963).
7. D. T. Blackstock, J. Acoust. Soc. Am., 34, 9-30 (1962).
8. D. T. Blackstock, "Approximate Equations Governing Finite-Amplitude Sound in Thermoviscous Fluids", AFOSR-5223, Suppl. Tech. Rept., Chapter 4 (May 1963).
9. D. T. Blackstock, J. Acoust. Soc. Am., 36, 217-219 (1964).
10. D. T. Blackstock, J. Acoust. Soc. Am., 39, 1019-1026 (1966).
11. D. T. Blackstock, J. Acoust. Soc. Am., 36, 534-542 (1964).
12. L. D. Landau, and E. M. Lifshitz, "Fluid Mechanics", (Addison-Wesley, New York 1959) pp. 47-49.
13. M. J. Lighthill, "Surveys in Mechanics", G. Batchelor and R. Davies, Eds. (Cambridge University Press, Cambridge, England 1956), pp. 250-351.
14. R. V. Khokhlov, REEP, 6, 817-824 (1961).
15. E. Hopf, Commun. Pure Appl. Math. 3, 201-230 (1950).
16. J. D. Cole, Quart. Appl. Math., 9, 225-236 (1951).
17. B. Riemann, "Gesammelte Mathematische Werke", H. Weber, Ed. (Dover Publications, New York 1953), pp. 156-175.
18. L. E. Hargrove, J. Acoust. Soc. Am., 32, 511-512 (1960).

19. E. Rubini, Alta Frequenza, 4, 530-581 (1935).

20. E. D. Banta, J. Math. Anal. Applications, 10, 166-173 (1965).

21. F. H. Fenlon, Ⓦ Research Laboratories, Scientific Paper 70-1C6-SONTR-P1 (1970).

22. P. J. Westervelt, "Proceedings of the Third International Congress on Acoustics", Stuttgart 1959, L. Cermer, Ed., (Elsevier Publishing Co. Inc., Amsterdam 1961), vol. 1, pp. 316-321.

23. R. D. Fay, J. Acoust. Soc. Am., 39, 222-241 (1931).

24. B. B. Cary, J. Acoust. Soc. Am., 43, 1364-1372 (1968).

25. B. V. Smith and H. O. Berktay (ref. 19, p. 38, in "Application of Finite-Amplitude Acoustics to Underwater Sound"; Navy Underwater Sound Lab, New London, Conn. 1968).

26. B. B. Cary, J. Acoust. Soc. Am., 42, 88-92 (1967).

27. F. H. Fenlon, Ⓦ Research Laboratories Scientific Paper 70-1C6-SONTR-P2 (1970).

28. H. Marsh, R. Mellen, and W. Konrad, J. Acoust. Soc. Am., 38, 326-338 (1965).

29. B. B. Cary and F. H. Fenlon, Brit. J. Sound & Vib., 13, 201-209 (1970).

30. B. D. Cook, J. Acoust. Soc. Am., 34, 941-946 (1962).

31. T. G. Muir and J. E. Blue, "Nonlinear Acoustics", (Proceedings of the 2nd Symposium on Nonlinear Acoustics, sponsored by ARL, Austin, Texas 1970; AD 719936) pp. 185-203.

32. P. J. Westervelt, J. Acoust. Soc. Am., 35, 535-537 (1963).